Histidine 52 Is a Critical Residue for Rapid Formation of Cytochrome *c* Peroxidase Compound I[†]

James E. Erman,[*,‡] Lidia B. Vitello,[‡] Mark A. Miller,[§] Andrew Shaw,[§] Katherine A. Brown,[§] and Joseph Kraut[§]

Departments of Chemistry, Northern Illinois University, DeKalb, Illinois 60115, and University of California at San Diego, La Jolla, California 92093

Received March 18, 1993; Revised Manuscript Received June 25, 1993[●]

ABSTRACT: The crystal structure and reactivity with hydrogen peroxide are reported for a mutant of a cloned cytochrome *c* peroxidase [CcP(MI)], in which the conserved distal His (His-52) is replaced with Leu. The reaction of the H52L enzyme with peroxide was examined as a function of pH in 0.1 M phosphate buffers and buffers in which nitrate was used to adjust the ionic strength. The pH-independent bimolecular rate constant for the reaction of H52L with peroxide was 731 ± 44 and 236 ± 14 $M^{-1}\ s^{-1}$ in phosphate and nitrate-containing buffers, respectively. This represents a 10^5-fold decrease in rate relative to the CcP(MI) parent under comparable conditions. Single-crystal diffraction studies showed that no dramatic changes in the structure or in the accessibility of the heme binding site were caused by the mutation. Rather, the mutation caused significant structural changes only at residue 52 and the nearby active-site water molecules. The residual reactivity of the H52L enzyme with peroxide was pH- and buffer-dependent. In nitrate-containing buffer, the apparent bimolecular rate constant for the reaction with peroxide *decreased* with decreasing pH; the loss of reactivity correlated with protonation of a group with an apparent $pK_A = 4.5$. Protonation of the group caused a loss of reactivity with peroxide. This is in contrast to the CcP(MI) parent enzyme, as well as all other mutants that have been examined, where the loss of reactivity correlates with protonation of an enzyme group with an apparent $pK_A = 5.4$. In phosphate buffer, the apparent bimolecular rate constant *increased* with decreasing pH, and protonation of a group with an apparent $pK_A = 4.2$ increased the apparent bimolecular rate constant to $(1.2 \pm 0.7) \times 10^4\ M^{-1}\ s^{-1}$. The results demonstrate that His-52 is crucial for the rapid reaction of CcP(MI) with peroxide; when this residue is replaced with Leu, the reactivity of the enzyme with peroxide is comparable to that of metmyoglobin. The results also suggest that protonation of His-52 in CcP(MI) causes the observed inactivation of the enzyme at acidic pH in nitrate-containing buffers. The effects of phosphate and nitrate-containing buffers on the reaction of H52L with peroxide provide evidence that the enzyme can be influenced by specific ion effects that do not involve changes in the protonation state of His-52.

Peroxidases are a class of heme proteins which utilize hydrogen peroxide to oxidize a wide variety of organic and inorganic compounds (Saunders *et al.*, 1964). The initial step in the catalytic mechanism is heterolysis of the oxygen–oxygen bond of hydrogen peroxide. This reaction causes the release of one water molecule (Schonbaum & Lo, 1972) and coordination of the second oxygen atom to the iron center (Hager *et al.*, 1972). Two electrons are transferred from the enzyme to the coordinated oxygen atom: one from the iron and one from a second donor. Typically the porphyrin serves as the second donor (Dolphin *et al.*, 1971; Dolphin & Felton, 1973), although in the case of cytochrome *c* peroxidase the second donor is Trp-191 (Erman *et al.*, 1989; Scholes *et al.*, 1989; Sivaraja *et al.*, 1989). The resulting enzyme intermediate is designated Compound I and possesses an oxy–ferryl (Fe(IV)═O) iron center and an organic free radical (George, 1952, 1953).

The ability to react rapidly with peroxides to form Compound I discriminates peroxidases from other classes of heme proteins. This characteristic reactivity must result entirely from the influence of the protein on the heme, since other proteins that possess the same protoporphyrin IX prosthetic group vary widely in their reactivity with peroxides. For example, while peroxidases react rapidly (~$10^7\ M^{-1}\ s^{-1}$) with peroxides over a wide pH range (Loo & Erman, 1975; Dolman *et al.*, 1975), metmyoglobin reacts some 10^5-fold more slowly (Yonetani & Schleyer, 1967).

In developing ideas about how protein structure modifies heme reactivity, comparisons between the crystal structures of yeast cytochrome *c* peroxidase and metmyoglobin have been widely used (Poulos *et al.*, 1980; Poulos & Finzel, 1984). Three residues have been suggested to increase the reactivity of CcP[1] with peroxide relative to metmyoglobin: His-52, Arg-48, and Asp-235 (Poulos & Kraut, 1980). His-52 and Arg-48 are located near the peroxide binding site. His-52 is suggested to function as a general acid/base catalyst that assists in deprotonating the approaching hydroperoxide molecule and in protonating the departing water after oxygen-oxygen bond cleavage. Arg-48 is proposed to stabilize the transition state for Compound I formation by interacting with the developing negative charge on the oxygen atom being reduced during the heterolytic cleavage of the peroxide oxygen-oxygen bond and to stabilize the resulting oxy–ferryl center of Compound I. Asp-235 interacts with the proximal imidazole ligand, which should increase the electron density on the iron, stabilizing the ferric and higher oxidation states of the enzyme.

[†] This work was supported in part by Research Grants PHS 1R15 DK43944 to L.B.V. and J.E.E. and NSF MCB 9119292 to J.K.

[*] Author to whom correspondence should be addressed.

[‡] Northern Illinois University.

[§] University of California at San Diego.

[●] Abstract published in *Advance ACS Abstracts*, September 1, 1993.

[1] Abbreviations: CcP, cytochrome *c* peroxidase; CcP(MI), recombinant cytochrome *c* peroxidase expressed in *Escherichia coli*; CcP(H52L), the His-52→Leu mutant of CcP(MI); CT1, long-wavelength (>600 nm) charge-transfer band in the electronic absorption spectrum of CcP.

0006-2960/93/0432-9798$04.00/0

This interaction should also promote cleavage of the oxygen-oxygen bond of the peroxide (Traylor & Popovitz-Biro, 1988). The importance of these residues is suggested by evidence that all three interactions are conserved among the peroxidases (Mazza & Welinder, 1980; Tien & Tu, 1987; Hashimoto *et al.*, 1986; Thanabal *et al.*, 1988).

In order to examine the role of active site residues in the catalytic function of CcP, we have begun to characterize the influence of mutations at Asp-235, Arg-48, and His-52 on the rate of reaction with hydrogen peroxide in a cloned CcP [CcP(MI); Fishel *et al.*, 1987]. Mutation of Asp-235 to Asn does not have a strong influence on the rate of reaction with peroxide (Vitello *et al.*, 1992), although the interaction between Asp-235 and the proximal imidazole base influences both the coordination state of the resting ferric enzyme (Smulevich *et al.*, 1988) and the formation of the Compound I radical (Fishel *et al.*, 1991). In fact, a strong proximal ligand may not be necessary for rapid reaction of CcP with peroxide (Sundaramoorthy *et al.*, 1991). On the other hand, replacing Arg-48 with Lys and Leu decreases the apparent bimolecular reaction rate with peroxide by ~2- and ~50-fold, respectively [see accompanying paper, Vitello *et al.* (1993)], indicating that a positive charge at position 48 does increase the rate of reaction, but its effect is much less than that of His-52 on the bimolecular rate constant for the CcP–hydrogen peroxide reaction.

The present work characterizes the kinetics and structure of a CcP(MI) mutant in which His-52 is replaced with Leu. This substitution decreases the rate of reaction with peroxide by a factor of 10^5 relative to the CcP(MI) parent. The apparent rate is substantially lower than the rate observed for the Arg-48→Leu substitution and is close to that reported for the reaction of metmyoglobin and hydrogen peroxide (Yonetani & Schleyer, 1967). The mutation also increases the rate of endogenous reduction of the oxy–ferryl center of Compound I by 2 orders of magnitude relative to yeast CcP (Erman & Yonetani, 1975b). We conclude that the distal histidine residue, His-52, plays a critical role in hydrogen peroxide activation by CcP(MI) and in stabilizing the oxidized intermediate, Compound I.

MATERIALS AND METHODS

Twice-crystallized CcP(H52L) was prepared as previously described (Fishel *et al.*, 1987; Smulevich *et al.*, 1991). Concentrations of the enzyme were determined spectroscopically in 0.1 M phosphate buffer, pH 6, using a millimolar absorptivity of 97 at 404 nm (Smulevich *et al.*, 1991). Hydrogen peroxide (30%, J. T. Baker Chemical Co.) was standardized with cerium(IV) sulfate according to the method of Kolthoff and Belcher (1957).

Crystals for X-ray diffraction studies were obtained under conditions identical to those for other CcP(MI) mutants (Wang *et al.*, 1990). Single large crystals were formed in 2–3 days at 4 °C by seeding with small crystals of the H52L enzyme (Thaller *et al.*, 1981). The H52L crystals were isomorphous with the original wild-type crystals (space group $P2_12_12_1$). X-ray diffraction data were collected on a Hamlin multiwire area detector (Cork *et al.*, 1973; Xuong *et al.*, 1985) and processed by a suite of programs distributed with the system (Anderson, 1987; C. Nielsen, unpublished work). Crystals were cooled to 4 °C using a wide stream of dry air. A total of 17 653 reflections, representing 95% of all unique data, were collected to 2.2 Å. The final R_{sym}[2] was 0.052.

Observed structure factors for the H52L mutant (F_{mut}) and wild-type enzyme (F_{wt}), with calculated phases (α_{calc}), were used as Fourier coefficients for the $2F_{\text{mut}} - F_{\text{wt}}, \alpha_{\text{calc}}$ and $F_{\text{mut}} - F_{\text{wt}}, \alpha_{\text{calc}}$ maps. The initial model of the H52L mutant was constructed by fitting a leucine residue at position 52 into these maps using the program TOM (version 3.2b with modifications by S. Dempsey at UCSD; Cambillau & Horjales, 1987; Jones, 1978) with an Iris 4D/340VGX graphics system. The TNT package of programs (version 4) was used for refinement. An intermediate *R*-factor of 0.176 was obtained for this model. In subsequent rounds of model building, solvent on the distal side of the heme was removed and rebuilt, and water-970 was added to the structure. Residues 2 and 3 were removed from the N-terminus of the structure, as little electron density was observed for these two residues. Additional modeling of minor solvent changes remote to the mutation site also proceeded. A final *R*-factor of 0.155 was obtained for data to 2.2-Å resolution. The root-mean-square deviation of bond lengths and bond angles from their dictionary values was 0.01 Å and 2.9°, respectively. Crystallographic coordinates have been submitted to the Brookhaven Data Bank under the name 5CCP.

Two buffer systems were used for the spectroscopic and kinetic studies. The first series was 10 mM in acetate or phosphate with added KNO_3 to adjust the ionic strength to 0.1 M. The second series of buffers was 0.1 M in total phosphate concentration. These latter buffers were made by mixing appropriate amounts of 0.1 M H_3PO_4, 0.1 M KH_2PO_4, and 0.1 M K_2HPO_4 while monitoring the pH. The 0.1 M phosphate buffers have low buffering capacity below pH 6, and, although their ionic strength is essentially constant between pH 4 and 6, the ionic strength of these buffers increases substantially between pH 6 and 8. The phosphate buffers were used to compare properties of CcP(H52L) with those of CcP(MI) and wild-type yeast CcP under identical experimental conditions since the reaction between CcP and hydrogen peroxide is significantly different in phosphate and in nitrate-containing buffers (Balny *et al.*, 1987; Vitello *et al.*, 1990b).

To investigate the pH-dependent properties of CcP(H52L), stock solutions of the enzyme were made in unbuffered 0.1 M KNO_3 (pH ~ 5.3) or 0.1 M KH_2PO_4 (pH ~ 4.5), depending upon the buffer system to be used. Small aliquots (less than 5% of the final volume) of stock enzyme were added to the desired buffer and the experiments performed. For those buffers which have low buffering capacity, the pH of the solution was measured before and after each experiment. Spectral properties of the enzyme were determined immediately after the enzyme was mixed into each buffer solution. Spectra were obtained at a scan rate of 1 nm/s with a Cary Model 219 spectrophotometer.

Depending upon the reaction rates, the hydrogen peroxide/enzyme reaction was monitored with the Cary Model 219 spectrophotometer or with a Hi-Tech Scientific Model PQ/SF-53 stopped-flow instrument. With both instruments, the reaction was maintained at 25 ± 1 °C using water-jacketed cells and a circulating water bath. The reactions were studied under pseudo-first-order conditions with hydrogen peroxide

---

[2] $R_{\text{sym}} = \sum_{hkl}(\sum_i |I_i - \bar{I}| / \sum_i I_i)$, where I_i is the observed intensity of the *i*th reflection, and $\bar{I}$ is the scaled mean intensity.

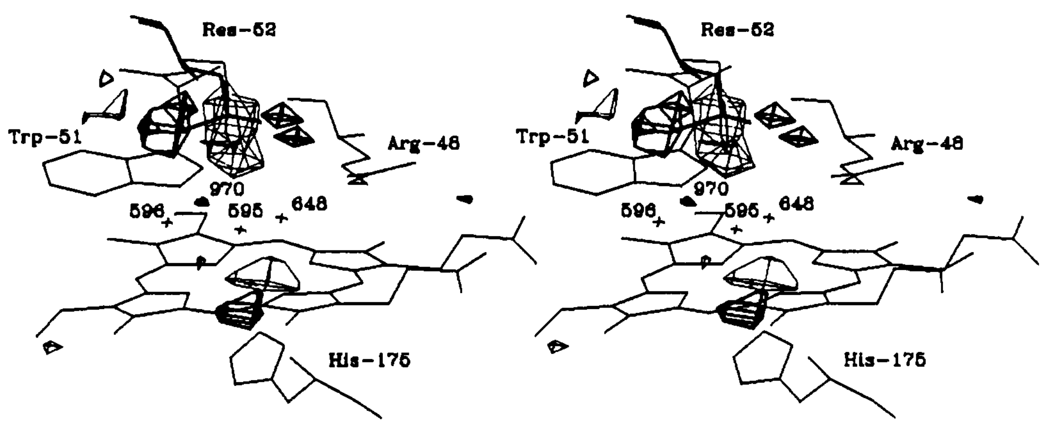

FIGURE 1: H52L minus wild-type CcP difference Fourier map contoured at ±4.0σ. Thin contour lines represent positive difference density; thick contour lines represent negative difference density. The Leu-52 residue and water-970 from the refined H52L structure (thick lines) are shown for comparison with His-52 and other local structures composing the peroxide binding site on the distal side of the heme in wild-type CcP (thin lines).

in excess. Enzyme concentrations ranged from 0.5 to 5 μM and hydrogen peroxide from 10 μM to 12.5 mM.

RESULTS

Crystallography of CcP(H52L). The difference electron density map for the H52L mutant (Figure 1) shows that the structural effects of the side-chain substitution are localized to the immediate vicinity of the mutation site. The strongest features on the map are near the side chain of residue 52 itself. A large peak of negative density is centered over ND1, CE1, and NE2 groups of the His-52 side chain. Positive peaks of electron density also flank this side chain, representing the presence of the CD1 and CD2 groups of the Leu-52 residue. Difference density also appears near the iron center of the heme, indicating a small positional shift in this atom toward the proximal histidine (residue 175). In addition, a small peak of positive density occurs near residue 52, approximately 2.0 Å from its NE2 group, in the solvent-filled peroxide binding pocket located on the distal side of the heme. This observation suggests that replacement of His-52 with the smaller, more apolar leucine side chain has slightly altered the structure of solvent in this region of the protein. Difference maps calculated later during the refinement process suggested that the peak of positive density represented a new solvent molecule (water-970) which could be modeled into the continuum of solvent density in this region of the structure. In the refined structure, the new solvent molecule, water-970, is located within close hydrogen bonding distance, 2.3–2.5 Å, of water-595 and water-445. Its position corresponds to the position of the positive density peak observed in the original electron difference density map (Figure 1), and its *B*-factor of 61 Å^2 compares well with the average B-factor of 56 Å^2 for the solvent at this site. Water-970 forms part of a somewhat disordered structure of solvent comprised principally of waters 595, 596, 648, and 445. Small subtle changes of these water molecules were observed upon refinement of the H52L structure; however, the magnitudes of the movements corresponded to no more than 0.2 Å, which is within the error limits of the structure.

Absorption Spectrum of CcP(H52L). The absorption spectrum of CcP(H52L) is dependent upon specific ion effects and the pH of the solution. The spectrum of the mutant enzyme in both 0.1 M phosphate and in nitrate-containing buffer at pH 6 is shown in Figure 2 and the spectral parameters are collected in Table I. The spectrum of the mutant enzyme is characteristic of a predominantly pentacoordinate high-spin heme enzyme in both buffer systems (see Discussion).

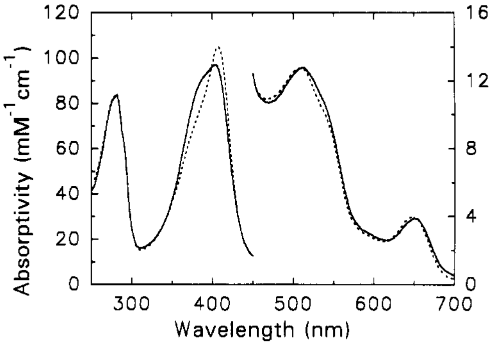

FIGURE 2: Spectrum of CcP(H52L) at pH 6.0. Solid line, 0.1 M potassium phosphate buffer. Dashed line, 10 mM potassium phosphate with KNO_3 added to adjust the ionic strength to 0.1 M.

The spectrum of CcP(H52L) shows small changes with pH in both buffer systems (Figure 3). In nitrate-containing buffers, the position of the Soret maximum is independent of pH between 4 and 8, but the ratio of the absorbance at the Soret maximum to that at 380 nm increases by about 11% on lowering the pH from 6 to 4. The variation of the Soret to 380 nm absorbance ratio can be fit to a titration curve involving a single ionization with an apparent pK_A of 5.2 ± 0.1 in nitrate buffers. This ionization is also associated with a blue shift in the long-wavelength charge-transfer band, CT1, from 649 nm at pH 6 to 645 nm at pH 4 and a decrease in the ratio of absorbance at CT1 to that at 620 nm from 1.55 at pH 6 to 1.4 at pH 4. Above pH 7, the CT1/620-nm absorbance ratio decreases due to conversion to a low-spin hydroxy form of CcP(H52L) at higher pH (Smulevich *et al.*, 1991), although this spin-state conversion is not evident in the position of the Soret maximum or the Soret/380 nm absorbance ratio up to pH 8 in nitrate-containing buffers (Figure 3).

The spectrum of CcP(H52L) in 0.1 M phosphate buffers varies to the greatest extent at the pH extremes. The changes occurring at the alkaline end of the pH range are due to formation of the low-spin hydroxy form of CcP(H52L). The apparent pK_A for the high-spin/low-spin transition in CcP(H52L) is 8.3 in 0.1 M phosphate buffer. The pK_A for the low pH transition cannot be determined from the available spectral data. Over the pH range investigated, the Soret maximum varies between a minimum value of 402 nm at pH 5 to a maximum value of 407 nm at pH 8. The ratio of the absorbance at the Soret maximum to that at 380 nm varies between a value of 1.13 at pH 5 to values of 1.23 and 1.31 at pH 4 and 8, respectively. The variation in the Soret to

Table I: Spectroscopic Parameters of CcP, CcP(MI), and CcP(H52L)[a]

protein	buffer	δ	Soret	CT2	β	α	CT1
CcP[b]	KNO_3	374 (57, sh)	408 (98)	506 (11.4)	544 (8.6, sh)	590 (3.3, sh)	646 (3.4)
CcP(MI)[b]	KNO_3	374 (61, sh)	408 (102)	508 (11.5)	540 (9.3, sh)	592 (2.3, sh)	644 (3.4)
CcP(H52L)	KNO_3	376 (67, sh)	407 (105)	509 (12.4)	545 (8.9, sh)	595 (2.9, sh)	649 (4.0)
CcP(H52L)	KPhos	379 (81, sh)	404 (97)	511 (12.7)	544 (9.8, sh)	595 (3.0, sh)	651 (4.0)

[a] pH 6.0. Wavelength maximum given in nanometers, followed by millimolar absorptivity in parentheses. [b] Vitello *et al.*, 1992.

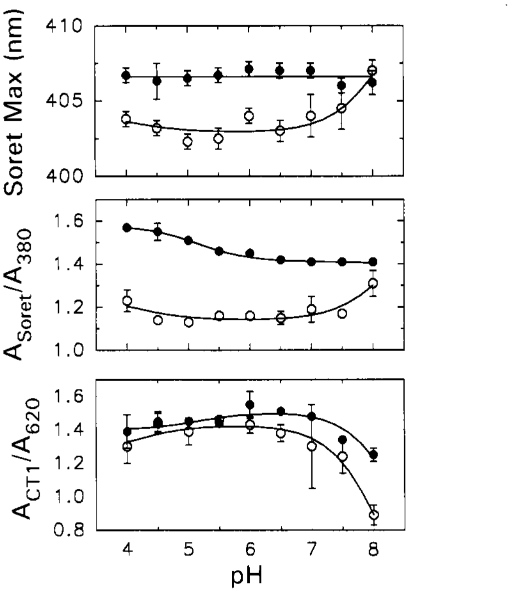

FIGURE 3: pH dependence of selected spectral parameters. Open circles, 0.1 M potassium phosphate buffer. Solid circles, 0.1 M ionic strength buffers using KNO_3. Upper panel, wavelength of the Soret maximum. Middle panel, ratio of the absorbance at the Soret maximum to that at 380 nm. Bottom panel, ratio of the absorbance at the maximum of CT1 to that at 620 nm. The solid lines are theoretical lines calculated on the assumption that there are three spectroscopically distinct forms depending upon the pH, an acidic form which is a mixed penta- and hexacoordinate high-spin species, a neutral form which is predominantly pentacoordinate, and a hexacoordinate low-spin form existing above pH 8.

380-nm absorbance ratio is accompanied by a reciprocal variation in the CT1 to 620-nm absorbance ratio.

Reaction between CcP(H52L) and Hydrogen Peroxide. When hydrogen peroxide is added to CcP(H52L), an increase in absorbance at 424 nm, attributed to Compound I formation, is observed (Figure 4). The absorbance increase is followed by a slow decrease in absorbance, which is due to the endogenous decay of Compound I (Erman & Yonetani, 1975a,b). The time dependence of the absorbance changes at pH 6 can be fit to a two-exponential function (eq 1). Under

$$\Delta A(t) = A_A \exp(-k_A t) + A_B \exp(-k_B t) \qquad (1)$$

pseudo-first-order conditions, with hydrogen peroxide in excess, k_A increases linearly with increasing peroxide concentration (between 10 and 600 μM), while the decay rate, k_B, is essentially independent of the peroxide concentration. Over the same concentration range, the value of k_B has an average value of (1.5 ± 0.4) x 10^{-3} s^{-1} for 11 determinations at pH 6.

The simplest interpretation of the data is the mechanism shown in eq 2. CcP·I represents Compound I, and CcP_{OX}

$$CcP + H_2O_2 \xrightarrow{k_1^{app}} CcP{\cdot}I \xrightarrow{k_{decay}} CcP_{ox} \qquad (2)$$

represents the product of Compound I decay. With yeast CcP, the endogenous decay of Compound I is associated with reduction of the Fe(IV) by tryptophan and tyrosine residues in the protein, resulting in a product with oxidized aromatic amino acid residues (Coulson & Yonetani, 1972; Spangler & Erman, 1986). The apparent bimolecular rate constant for Compound I formation, k_1^{app}, can be determined from the slope of plots of the observed rate constant, k_A, *versus* the hydrogen peroxide concentration, while the Compound I decay rate, k_{decay}, is identical to that of the slower observed rate constant, k_B.

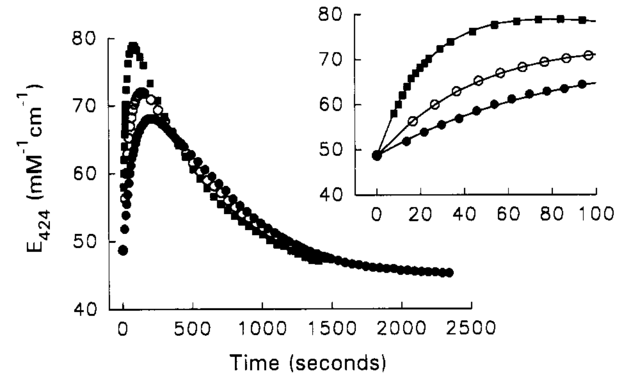

FIGURE 4: Absorbance change at 424 nm (normalized by dividing by the enzyme concentration) upon mixing hydrogen peroxide and CcP(H52L) at pH 6.0 in 0.1 M potassium phosphate. Hydrogen peroxide concentration: 11.4 μM (●); 22.5 μM (○); 54.3 μM (■). The CcP(H52L) concentration was 3.49 ± 0.09 μM.

The rate of CcP(H52L) Compound I formation is significantly slower in nitrate-containing buffers compared to that in phosphate buffers. About 10 times higher concentrations of hydrogen peroxide were necessary with nitrate buffers in order to obtain values of k_A comparable to those in phosphate buffers. In nitrate-containing buffers, plots of k_A *versus* hydrogen peroxide generally had positive values of the intercept at zero hydrogen peroxide. We believe that the positive intercepts are related to the coupling of the rates of formation and decay of Compound I at low peroxide concentrations, where the rates are similar.

pH Dependence of k_1^{app}. The apparent bimolecular rate constant for the reaction between hydrogen peroxide and CcP(H52L) is dependent upon pH in both buffer systems used in this study (Figure 5). We can fit the pH dependence of k_1^{app} by assuming that a single enzyme ionization influences the hydrogen peroxide reaction:

$$HCcP \overset{K_{E1}}{\rightleftarrows} CcP + H^+ \qquad (3a)$$

$$HCcP + H_2O_2 \xrightarrow{k_{1A}} CcP{\cdot}I \qquad (3b)$$

$$CcP + H_2O_2 \xrightarrow{k_{1B}} CcP{\cdot}I \qquad (3c)$$

$$k_1^{app} = (k_{1A} + k_{1B}K_{E1}/[H^+])/(1 + K_{E1}/[H^+]) \qquad (3d)$$

Nonlinear least-squares regression was used to obtain best-fit values for k_{1A}, k_{1B}, and K_{E1}, which are given in Table II and were used to calculate the solid lines in Figure 5.

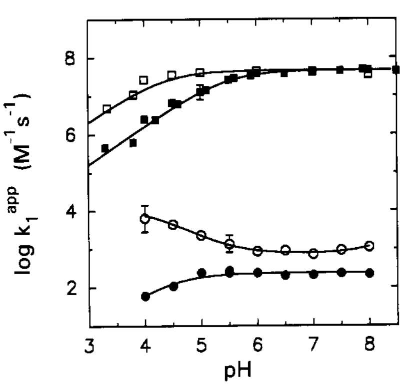

FIGURE 5: pH dependence of the logarithm of k_1^{app} for the hydrogen peroxide/enzyme reaction as a function of pH. Yeast CcP in nitrate-containing buffers (■). Yeast CcP in 0.1 M potassium phosphate (□). CcP(H52L) in nitrate-containing buffers (●). CcP(H52L) in 0.1 M potassium phosphate (○).

Table II: Kinetic Parameters for the Reaction between CcP Species and Hydrogen Peroxide[a]

species	buffer	k_{1A}	k_{1B}	pK_{E1}
CcP[b]	KNO_3	0	$(4.5 \pm 0.3) \times 10^7$	5.4 ± 0.1
CcP	KPhos	0	$(4.7 \pm 0.4) \times 10^7$	4.0 ± 0.1
CcP(H52L)	KNO_3	0	236 ± 14	4.5 ± 0.1
CcP(H52L)	KPhos	$(1.2 \pm 0.7) \times 10^4$	731 ± 44	4.2 ± 0.3

[a] Parameters defined in eq 3 of the text. [b] Loo & Erman, 1975.

pH Dependence of k_{decay}. Although we have not carried out a comprehensive study of the decay of CcP(H52L) Compound I, we have measured the rates of decay at a number of different conditions in conjunction with the studies on the rate of Compound I formation. The decay of Compound I appears to be independent of the hydrogen peroxide concentration above pH 5.5. Below pH 5.0, the decay rate increases linearly with increasing hydrogen peroxide concentration. The decay rate also depends upon the pH and the nature of the buffer. In 0.1 M phosphate buffer, the decay appears to be monophasic except at pH 4, where two phases, with rates differing by a factor of 5, are observed. The faster of the two decay phases accounted for about 80% of the reaction amplitude. In nitrate-containing buffers, biphasic decay kinetics were observed at pH 4.5, 5.5, and 8.0. At all three pH values, the fast phase was about 6 times faster than the slow phase and accounted for about 60% of the reaction amplitude.

The observed rates for the largest amplitude phase of the CcP(H52L) Compound I decay reaction are shown as a function of pH in Figure 6 for both buffer systems. The decay rates for yeast CcP are shown for comparison. In phosphate buffer, the ratio of the decay rates for CcP(H52L) Compound I to that for yeast CcP Compound I varies from 2.3 at pH 8 to 580 at pH 4. On the average, CcP(H52L) Compound I decays 130-fold faster than yeast CcP Compound I in phosphate buffer and 66-fold faster than that in nitrate-containing buffers.

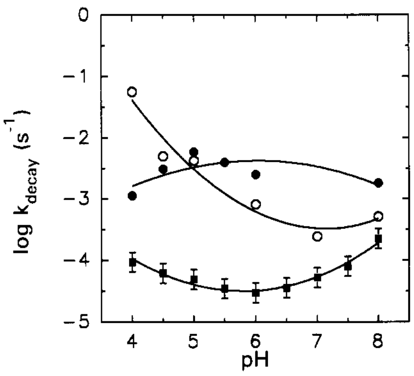

FIGURE 6: pH dependence of the minimum observed Compound I decay rate. CcP(H52L) compound I in 0.1 M potassium phosphate (○). CcP(H52L) compound I in nitrate-containing buffer (●). CcP Compound I in nitrate-containing buffer (■) (Erman & Yonetani, 1975b). The lines have no theoretical significance.

DISCUSSION

The coordination state of wild-type yeast CcP and its influence on the reactivity of the enzyme have been the subject of much discussion. The crystallographic structure shows a water 2.4 Å from the heme iron in CcP (Finzel *et al.*, 1984) and 2.7 Å from the heme iron in CcP(MI) (Wang *et al.*, 1990). The consensus from resonance Raman studies is that native yeast CcP is predominantly pentacoordinate over the pH range from 4–8 in phosphate and zwitterionic buffers (Smulevich *et al.*, 1988, 1989; Dasgupta *et al.*, 1989). The appearance of a hexacoordinate high-spin form at the expense of the pentacoordinate form has been noted, however, and the relative amount of the hexacoordinate form depends upon pH, buffer, and sample history. Mutations in the vicinity of the active site can also increase the fraction of the enzyme that is hexacoordinate (Smulevich *et al.*, 1988; Vitello *et al.*, 1992). A minimum of two substates must therefore exist:[3] a pentacoordinate high-spin form with no interaction between the heme iron and the water molecule located in the heme pocket and a hexacoordinate high-spin form with water clearly bound to the heme iron, such as in metmyoglobin.

The appearance of hexacoordinate CcP has been correlated with the appearance of a relatively unreactive form of CcP (Balny *et al.*, 1987). On this basis, it was suggested that protonation of His-52 leads to the coordination of a water molecule to the sixth coordination site and that occupation of the sixth coordination by the water molecule caused the slow reaction with peroxide (Balny *et al.*, 1987). It was subsequently shown that the appearance of the unreactive form of the enzyme at acidic pH is not linked to coordination of water to the iron (Vitello *et al.*, 1990b). As discussed below, the pH dependence of the coordination state and reactivity of the H52L mutant reported here suggests that protonation of His-52 does produce an unreactive form of the enzyme in nitrate buffers but does not cause the formation of the hexacoordinate aquo enzyme.

Coordination State of the Heme in CcP(H52L). Previous work from this lab has employed the electronic absorption spectrum as a probe of events that occur at the heme site in CcP and its mutants (Vitello *et al.*, 1990a,b, 1992). The electronic absorption spectrum is quite sensitive to changes in heme ligation and is well suited to quantitating small changes in the subpopulations of the enzyme. High-spin species are characterized by Soret bands below 410 nm and ligand-to-metal charge transfer bands above 600 nm. Pentacoordinate forms are characterized by a prominent shoulder (the δ band) near 380 nm in the Soret region and a CT1 band above 640

---

[3] In fact, it is likely that a number of substates exist. Although resonance Raman studies suggest a completely pentacoordinate enzyme, NMR studies suggest that the water must interact, to some extent, with the heme iron through direct coordination (La Mar *et al.*, 1988). The crystallographic structure shows water molecules 2.4 and 2.7 Å from the heme iron in yeast CcP and CcP(MI), respectively (Finzel *et al.*, 1984; Wang *et al.*, 1990). These water molecules have high crystallographic *B*-factors relative to solvent in other crystal structures, consistent with high thermal mobility and/or low occupancy at the assigned positions.

nm. Hexacoordinate high-spin forms have a less prominent δ band and a Soret band with higher molar absorptivity than the pentacoordinate form. The ratio of the absorptivity at the Soret maximum relative to that at 380 nm and that of the CT1 band to that at 620 nm, as well as the position of the CT1 band, can be used to characterize changes in heme ligation. Pentacoordination is characterized by a small value of the Soret/380-nm absorbance ratio and a large value of the CT1/620 nm absorbance ratio, *i.e.*, the absorbance ratios have a reciprocal relationship.

At pH 6, the Soret/380-nm absorptivity ratios are 1.16 and 1.45 for CcP(H52L) in phosphate and nitrate-containing buffers, respectively, Figure 3. The corresponding values for CcP and CcP(MI) are 1.51 and 1.53, respectively, at pH 6, independent of buffer (Vitello *et al.*, 1990a,b). The Soret/380-nm absorbance ratio for CcP(H52L) in phosphate buffer is the smallest value so far observed for high-spin CcP species, suggesting that the pentacoordinate form is more highly favored in this mutant than any of the other CcP species so far investigated. A comparison of the Soret/380-nm ratio for CcP(H52L) in the two buffer systems used in this study indicates that the mutant enzyme has increased hexacoordination in nitrate-containing buffers relative to phosphate. In addition, the small increases in the Soret/380-nm absorbance ratio as the pH is lowered from 6 to 4 also suggests that hexacoordinate high-spin species are formed at low pH in both buffer systems described in this study, as well as in 0.1 M succinate buffer (not shown). Small amounts of hexacoordinate high-spin species were also observed in resonance Raman studies of CcP(H52L) at pH 5 in 0.1 M acetate and 0.1 M citrate buffers (Smulevich *et al.*, 1991). The Soret/380-nm and CT1/620-nm absorbance ratios show reciprocal variations with pH as expected for changes in heme ligation. The data indicate that despite the loss of a titrating residue at position 52, the increase in the hexacoordinate form in nitrate buffers corresponds to titration of a residue with an apparent $pK_A = 5.2$. The persistence of these effects in the H52L mutant shows that the appearance of the hexacoordinate high-spin form cannot be related to protonation of His-52.

Crystal Structure of CcP(H52L). The results of the single crystal diffraction experiments clearly show that replacement of His-52 with a leucine side chain does not block access to the heme iron. The relatively small conformational differences between H52L and the wild-type structure originate near residue 52 and result in only small changes in the solvent structure located in the peroxide binding pocket on the distal side of the heme. The slight alteration of the solvent structure appears to be related to the loss of the hydrogen-bonding capability of the NE2 group of the wild-type His-52 and the slight enlargement of the peroxide binding pocket arising from substitution with the smaller Leu-52 side chain. Concomitant with this apparent increase in solvent density in the distal pocket, a small but significant shift in the position of the heme iron toward proximal His-175 is observed. This result is consistent with the absorption spectra, which indicate an increase in the pentacoordinate high-spin form of the enzyme at the expense of the hexacoordinate high-spin form.

The differences in solvent structure between wild-type enzyme and CcP(H52L) illustrate the importance of the hydrogen-bonding pattern of His-52 and its relevance in hydrogen peroxide activation. In wild-type enzyme, ND1 of His-52 is hydrogen-bonded to the side chain carbonyl oxygen of Asn-82, forcing NE2 of His-52 to act as a hydrogen bond acceptor for ligands (including hydrogen peroxide) approaching the heme iron (Edwards *et al.*, 1984; Edwards & Poulos, 1990). In this orientation, His-52 acts as a general base, accepting a proton from the incoming hydrogen peroxide, allowing the peroxide anion to bind to the heme iron.

Hydrogen Peroxide/CcP(H52L) Reaction. The most dramatic effect of the His-52 to leucine mutation is the 5 orders of magnitude decrease in the rate of Compound I formation in the neutral pH region, pH 6–8 (Figure 5). Values for the pH-independent bimolecular rate constant for the CcP(H52L)/hydrogen peroxide reaction are 240 ± 14 and 730 ± 44 M^{-1} s^{-1} in nitrate-containing and phosphate buffer, respectively, compared to $(4.5 \pm 0.3) \times 10^7$ M^{-1} s^{-1} for yeast CcP and CcP(MI), Table II. The values for the CcP(H52L)/hydrogen peroxide reaction are similar to those for the reaction of water-soluble Fe(III) tetraphenylporphyrins with hydrogen peroxide (Bruice, 1991) and for the reaction between metmyoglobin or methemoglobin and hydrogen peroxide (Dalziel & O'Brien, 1954; George & Irvine, 1956; Yonetani & Schleyer, 1967; Fox *et al.*, 1974). This strongly suggests that His-52 is *the* critical residue in accelerating the reaction between CcP and hydrogen peroxide.

On the basis of these findings, it is possible to assert that in the H52L mutant, the conserved active-site residues Arg-48 and Asp-235 cannot accelerate the bimolecular reaction with hydrogen peroxide above the rate observed for myoglobin. However, since both myoglobin and CcP possess a histidine residue near the peroxide binding site, one cannot conclude that the distal histidine alone is sufficient to promote rapid heterolytic cleavage of peroxides. It is possible that either Arg-48 or Asp-235 accelerates the reaction with peroxide relative to that observed for metmyoglobin when His-52 is present to serve as a general base catalyst. It is also possible that catalysis by the distal imidazole is governed by very strict steric constraints which are not satisfied in metmyoglobin.

The failure of CcP to exhibit rapid heterolysis in the absence of His-52 can be rationalized as a requirement for a general base catalyst in the active site. The kinetic evidence describing Compound I formation predicts the formation of an iron–peroxy anion complex that subsequently breaks down to give Compound I and water (Jones & Dunford, 1977). In such a mechanism, the reaction rate can be increased by making formation of the iron–peroxy anion complex more favorable or by increasing the rate of O–O bond scission. A general base catalyst such as His-52 would favor the formation of the iron-peroxy anion complex, since deprotonation of the neutral hydroperoxide would increase the nucleophilicity of the substrate. This type of function for His-52 would explain the ability of the enzyme to elevate the reactivity of the neutral hydroperoxide molecule to a level comparable to that of the peroxy anion (Nakamura *et al.*, 1963). It would also account for the pH independence of the peroxide reaction over a wide range of pH (Vitello *et al.*, 1990b). The rate of reaction of CcP with peroxy acids is known to increase with increasing nucleophilicity of the substrate anion, also consistent with deprotonation of the substrate in the active site prior to attack of the anion on the iron (Frew & Jones, 1983). The loss of His-52 would eliminate deprotonation of the approaching anion, thus making the substrate substantially less effective in forming the iron–peroxy complex.

Evidence for general base catalysis in the cleavage of O–O bonds by model heme compounds has been reported (Bruice, 1991; Traylor & Xu, 1990; Traylor & Ciccone, 1989). It is interesting to note that heterolytic cleavage of peroxides is catalyzed by nitrogen bases under certain circumstances ($k \sim 10^5$ M^{-2} s^{-1}). These results have been used to predict that the transition state for catalysis of the reaction by collidine involves proton transfer to the base catalyst prior to O–O bond cleavage, similar to that suggested for CcP (Bruice, 1991; Traylor & Ciccone, 1989).

Specific Ion Effects and the pH Dependence of the CcP/Hydrogen Peroxide Reaction. It is clear from the present results that loss of His-52 dramatically decreases the rate of reaction with peroxide. A final question that remains to be resolved is whether or not protonation of His-52 is responsible for the decrease in the rate of the peroxide reaction at acidic pH in nitrate-containing buffers. The reaction between yeast CcP and hydrogen peroxide is dependent upon both the pH of the solution and the nature of the buffer (Figure 5). In nitrate-containing buffers, CcP reacts with hydrogen peroxide when a group associated with the enzyme is unprotonated. The apparent pK_A for the group is 5.4 in buffers using potassium nitrate to adjust the ionic strength to 0.1 M (Loo & Erman, 1975). Within experimental error, the protonated form of the enzyme is unreactive toward peroxide. We estimate that the upper limit for the rate constant between the acidic form of CcP and hydrogen peroxide is 5 x 10^4 M^{-1} s^{-1}. Values larger than this would be apparent in the pH–rate profile (Figure 5). In 0.1 M phosphate buffers, the reactivity of the unprotonated enzyme is the same as in nitrate-containing buffers, but the apparent pK_A of the critical group shifts to 4.0 ± 0.1.

We have previously shown that the critical catalytic group is not one of the heme propionate groups (Dowe & Erman, 1982), nor is it associated with Asp-235, the carboxylate group that interacts with the proximal histidine (Vitello *et al.*, 1992). We have hypothesized that the critical residue is His-52 and that nitrate binding within the heme pocket stabilizes the protonated, unreactive form of His-52, shifting the apparent pK_A from 4.0 in the absence of nitrate to 5.4 in the presence of 90 mM nitrate. On the basis of this hypothesis, we anticipated that a mutant lacking His-52 would react with hydrogen peroxide with a rate constant less than 5 x 10^4 M^{-1} s^{-1} (the upper limit for CcP lacking the critical basic group) and that the rate would be independent of pH. The rate constant for the CcP(H52L)/hydrogen peroxide reaction is less than 5 x 10^4 M^{-1} s^{-1} but the reaction is still dependent upon the pH, contrary to expectation.

Two observations may be relevant to the pH dependence of the CcP(H52L)/hydrogen peroxide reaction. First, the CcP(H52L)/hydrogen peroxide reaction is faster in phosphate buffers than in nitrate-containing buffers over the entire pH region investigated rather than just at acidic pH as observed for yeast CcP (Figure 5). Second, the reaction is *faster* at low pH in phosphate buffer. One explanation for these observations may be that phosphate binds in the distal heme pocket and that the bound phosphate anion functions as a base catalyst. Both mono- and dibasic phosphate anions are better bases than nitrate, and both could facilitate binding of the peroxide. The susceptibility of the hydrogen peroxide reaction to general base catalysis and the acid–base properties of phosphate relative to nitrate provide a reasonable explanation for the enhancement of the reaction in phosphate buffer and the increase in the reaction rate at low pH in phosphate buffer.

The decrease in the CcP(H52L)/hydrogen peroxide rate at low pH in nitrate-containing buffer (Figure 5) is more difficult to resolve. The decrease in reactivity of CcP(H52L) in nitrate buffers is associated with an apparent pK_A of 4.5, about 1 pH unit less than the apparent ionization observed in yeast CcP. If the apparent ionizations in CcP and CcP(H52L) are due to the same group, then His-52 must be eliminated as the source of the pH 5.4 transition in yeast CcP.

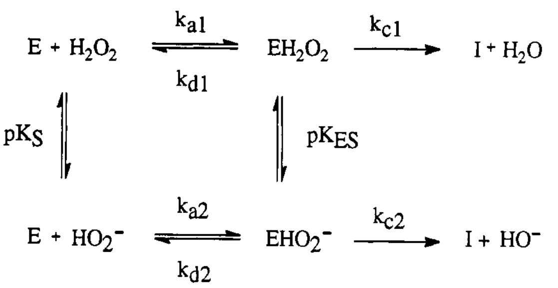

FIGURE 7: Mechanism for CcP(H52L) Compound I formation in nitrate-containing buffer.

This presents somewhat of a problem since the most obvious basic groups in the heme vicinity have been eliminated as the source of the pH 5.4 transition, including the heme propionates, Asp-235, and now His-52. Arg-48 and His-175 (in the absence of the Asp-235 interaction) are unlikely to undergo protonation/deprotonation between pH 4 and 5.5.

The decomposition of hydrogen peroxide by water-soluble Fe(III) tetraphenylporphyrins is pH-dependent with an apparent ionization near pH 6 (Bruice, 1991). The pH dependence is attributed to ionization of the bound hydrogen peroxide, producing bound peroxide anion, which is easier to reduce than the neutral form. In an analogous manner, we attribute the pK_A = 4.5 transition in the reaction of hydrogen peroxide and CcP(H52L) in nitrate buffer to the ionization of bound hydrogen peroxide (Figure 7). We assume that the ionization of hydrogen peroxide is in rapid equilibrium, in both the free and the bound forms, and that the enzyme/peroxide complexes are in a steady state during Compound I formation. Using the steady-state approximation, the apparent bimolecular reaction is given by the expression shown in eq 4:

$$k_1^{\text{app}} = \frac{(k_{c1}[H^+] + k_{c2}K_{ES})(k_{a1}[H^+] + k_{d2}K_s)}{((k_{c1} + k_{d1})[H^+] + (k_{c2} + k_{d2})K_{ES})([H^+] + K_s)} \tag{4}$$

We can simplify the expression in eq 4 by using approximate values for various rate and equilibrium constants. CcP binds neutral ligands in preference to their anionic forms (Erman, 1974a,b; Lent *et al.*, 1976), and we believe that k_{a1} is greater than k_{a2}. K_S is on the order of 10^{-12}, which, combined with the conclusion that k_{a1} is greater that k_{a2}, means that the ratio of the terms involving K_S in eq 4 reduces to k_{a1}. The data for the CcP(H52L)/hydrogen peroxide reaction in nitrate-containing buffers suggest that k_{c1} is negligible, and we set it equal to 0. Using these considerations, k_1^{app} reduces to the expression shown in eq 5:

$$k_1^{\text{app}} = \frac{k_{a1}k_{c2}K_{ES}}{k_{d1}[H^+] + (k_{c2} + k_{d2})K_{ES}} \tag{5}$$

At high pH, k_1^{app} has the value of $k_{a1}k_{c2}/(k_{c2}+k_{d2})$, and at low pH, k_1^{app} approaches 0. The apparent pK_A is equal to $K_{ES}(k_{c2}+k_{d2})/k_{d1}$. The apparent p$K_A$ is related to the ionization of bound peroxide, K_{ES}, but modified by the kinetics of the reaction.

Binding of peroxide to the heme iron promotes ionization of peroxide by many orders of magnitude. One can use the effect on water ionization as a guide since the acid–base properties of water and hydrogen peroxide are similar. Ionization of heme-bound water in metmyoglobins and methemoglobin is generally between pH 7 and 9 (Antonini & Brunori, 1971), and the pK_A for ionization of water bound to the ferric ion in aqueous solution is about 2.2 (George *et* *al.*, 1961). An apparent pK_A near 4.5 is not unreasonable for the ionization of heme-bound hydrogen peroxide, especially since the apparent ionization constant is affected by the kinetics of peroxide reduction.

If ionization of heme-bound hydrogen peroxide is responsible for the apparent pK_A of 4.5 in CcP(H52L), can this ionization be responsible for the apparent pK_A of 5.4 observed in the reaction of yeast CcP with hydrogen peroxide (Loo & Erman, 1975)? The answer is no. The binding of both fluoride and cyanide are influenced by the pK_A 5.4 transition (Erman, 1974a,b; Lent *et al.*, 1976). The ionization in wild-type emzyme has to be associated with the free enzyme, not a substrate or ligand ionization.

Alternative explanations for the pH dependence of the CcP(H52L)/hydrogen peroxide reaction in both phosphate and nitrate-containing buffers are possible. Conformational changes are known to occur in the protein at low pH (Satterlee & Erman, 1980; Vitello *et al.*, 1992). These changes could be triggered by enzyme ionizations remote from the heme site and could influence the rate and extent of peroxide binding to the heme iron. The spectrum of CcP(H52L) suggests some alteration in heme ligation at low pH in both phosphate and nitrate-containing buffers (Figure 3). The apparent pK_A for the spectroscopic transition in nitrate-containing buffer is about 5.2, while the apparent pK_A for the peroxide reaction is 4.5. These differences could be attributed to modification of the apparent ionization by the kinetics of peroxide reduction as discussed above.

Our best interpretation of the data is that the pK_A 5.4 transition in yeast CcP and CcP(MI) is due to His-52 ionization, with the basic form of the distal histidine functioning as a base catalyst, promoting reaction with hydrogen peroxide by 5 orders of magnitude. In the absence of His-52, the reaction with peroxide is so slow that other effects, such as ionization of the bound peroxide, catalysis by bound phosphate, and conformational alterations in the protein, can influence the reaction rate.

REFERENCES

Anderson, D. H., (1987) Ph.D. Thesis, University of California, San Diego, La Jolla, CA.

Antonini, E., & Brunori, M. (1971) in *Hemoglobin and Myoglobin in Their Reactions with Ligands*, pp 47–48, North-Holland Publishing Co., Amsterdam.

Balny, C., Anni, H. S., & Yonetani, T. (1987) *FEBS Lett. 221*, 349–354.

Bruice, T. C. (1991) *Acc. Chem. Res. 24*, 243–249.

Cambillau, C., & Horjales, E. (1987) *J. Mol. Graphics 5*, 174–177.

Chance, B., DeVault, D., Legallis. V., Mela, L., & Yonetani, T. (1967) in *Fast Reactions and Primary Processes in Chemical Kinetics* (Claesson, S., Ed.) pp 437–464, Interscience, New York.

Cork, C., Fehr, D., Hamlin, R., Vernon, W., Xuong, N.-H., & Perez-Mendez, V. (1973) *J. Appl. Crystallogr. 7*, 319–325.

Coulson, A. F. W., & Yonetani, T. (1972) *Biochem. Biophys. Res. Commun. 49*, 391–398.

Dalziel, K., & O'Brien, J. R. P. (1954) *Biochem. J. 56*, 648–659.

Dasgupta, S., Rousseau, D. L., Anni, H., & Yonetani, T. (1989) *J. Biol. Chem. 264*, 654–662.

Dolman, D., Newell, G. A., Thurlow, M. D., & Dunford, H. B. (1975) *Can. J. Biochem. 53*, 495–502.

Dolphin, D., & Felton, R. H. (1974) *Acc. Chem. Res. 7*, 26–32.

Dolphin, D., Forman, A., Borg, D. C., Fajer, J., & Felton, R. H. (1971) *Proc. Natl. Acad. Sci. U.S.A.* 68, 614–618.

Dowe, R. J., & Erman, J. E. (1982) *J. Biol. Chem. 257*, 2403–2405.

Edwards, S. L., & Poulos, T. L. (1990) *J. Biol. Chem. 265*, 2588–2595.

Edwards, S. L., Poulos, T. L., & Kraut, J. (1984) *J. Biol. Chem. 259*, 12984–12988.

Erman, J. E. (1974a) *Biochemistry 13*, 34–39.

Erman, J. E. (1974b) *Biochemistry 13*, 39–44.

Erman, J. E., & Yonetani, T. (1975a) *Biochim. Biophys. Acta 393*, 343–349.

Erman, J. E., & Yonetani, T. (1975b) *Biochim. Biophys. Acta 393*, 350–357.

Erman J. E., Vitello, L. B., Mauro, J. M., & Kraut, J. (1989) *Biochemistry 28*, 7992–7995.

Erman, J. E., Vitello, L. B., Miller, M. A., & Kraut, J. (1992) *J. Am. Chem. Soc. 114*, 6592–6593.

Finzel, B. C., Poulos, T. L., & Kraut, J. (1984) *J. Biol. Chem. 259*, 13027–13036.

Fishel, L. A., Villafranca, J. E., Mauro, J. M., & Kraut, J. (1987) *Biochemistry 26*, 351–360.

Fishel, L. A., Farnum, M. F., Mauro, J. M., Miller, M. A., Kraut, J., Liu, Y., Tan, X., & Scholes, C. P. (1991) *Biochemistry 30*, 1986–1996.

Fox, J. B.,Jr., Nicholas, R. A., Ackerman, S. A., & Swift, C. E. (1974) *Biochemistry 13*, 5178-5186.

Frew, J. E., & Jones, P. (1983) *Biochim. Biophys. Acta 742*, 1–8.

George, P. (1952) *Nature (London) 169*, 612–613.

George, P. (1953) *Biochem. J. 54*, 267–276.

George, P., & Irvine, D. H. (1956) *J. Colloid Sci. 11*, 327–336.

George, P., Beetlestone, J., & Griffith, J. S. (1961) in *Haematin Enzymes* (Falk, J. E., Lemberg, R., & Morton, R. K., Eds.) Pergamon Press, London, 105–139.

Hager, L. P., Doubek, D. L., Silverstein, R. M., Harges, J. H., & Martin, J. C. (1972) *J. Am. Chem. Soc. 94*, 4364–4366.

Hashimoto, S., Teraoka, J., Inubushi, T., Yonetani, T., & Kitagawa, T. (1986) *J. Biol. Chem. 261*, 11110–11118.

Jones, P., & Dunford, H. B. (1977) *J. Theor. Biol. 69*, 457–470.

Jones, T. A. (1978) *J. Appl. Crystallogr. 11*, 268–272.

Kolthoff, I. M., & Belcher, R. (1957) in *Volumetric Analysis*, Vol. III, pp 75–76, Interscience, New York.

La Mar, G. N., Chatfield, M. J., Peyton, D. H., de Ropp, J. S., Smith, W., Krishnamoorthi, R., Satterlee, J. D., and Erman, J. E. (1988) *Biochim. Biophys. Acta 956*, 267–276.

Lent, B., Conroy, C. W., & Erman, J. E. (1976) *Arch. Biochem. Biophys. 177*, 56–61.

Loo, S., & Erman J. E. (1975) *Biochemistry 14*, 3467–3470.

Mazza, G., & Welinder, K. G. (1980) *Eur. J. Biochem. 108*, 481–489.

Nakamura, Y., Tohjo, M., & Shibata, K. (1963) *Arch. Biochem. Biophys. 102*, 144–151.

Poulos, T. L., & Kraut, J. (1980) *J. Biol. Chem. 255*, 8199–8205.

Poulos, T. L., & Finzel, B. C. (1984) *Pept. Protein Rev. 4*, 115–171.

Poulos, T. L., Freer, S. T., Alden, R. A., Edwards, S. L., Skogland, U., Takio, K., Eriksson, B., Xuong, N. H., Yonetani, T., & Kraut, J. (1980) *J. Biol. Chem. 255*, 575–580.

Satterlee, J. D. & Erman, J. E. (1980) *Arch. Biochem. Biophys. 202*, 608–616.

Saunders, B. C., Holmes-Siedle, A. C., & Stark, P. (1964) in *Peroxidase*, Butterworths, London.

Scholes, C. P., Liu, Y., Fishel, L. A., Farnum, M. A., Mauro, J. M., & Kraut, J. (1989) *Isr. J. Chem. 29*, 85–92.

Schonbaum, G. R., & Lo, S. (1972) *J. Biol. Chem. 247*, 3353–3360.

Sivaraja, M., Goodin, D. B., Mauk, A. G., Smith, M., & Hoffman, B. A. (1989) *Science 245*, 738-740.

Smulevich, G., Mauro, J. M., Fishel, L. A., English, A. M., Kraut, J., & Spiro, T. G. (1988) *Biochemistry 27*, 5477–5485.

Smulevich, G., Mantini, A. R., English, A. M., & Mauro, J. M. (1989) *Biochemistry 28*, 5058-5064.

Smulevich, G., Miller, M. A., Kraut, J., & Spiro, T. (1991) *Biochemistry 30*, 9546–9558.

Spangler, B. D., & Erman, J. E. (1986) *Biochim. Biophys. Acta 872*, 155–1576.

Sundaramoorthy, M., Choudhury, K., Edwards, S. L., & Poulos, T. L. (1991) *J. Am. Chem. Soc. 113*, 7755–7757.

Thaller, C., Weaver, L. H., Eichele, G., Wilson, E., Karlsson, R., & Jansonius, J. N. (1981) *J. Mol. Biol. 147*, 465–469.

Thanabal, V., deRopp, J. S., & La Mar, G. N. (1988) *J. Am. Chem. Soc. 110*, 3027–3035.

Tien, M., & Tu, C.-P. (1987) *Nature 326*, 520–523.

Traylor, T. G., & Popovitz-Biro, R. (1988) *J. Am. Chem. Soc. 110*, 239–243.

Traylor, T. G., & Ciccone, J. P. (1989) *J. Am. Chem. Soc. 111*, 8413–8420.

Traylor, T. G., & Xu, F. (1990) *J. Am. Chem. Soc. 112*, 178–186.

Vitello, L. B., Erman, J. E., Mauro, J. M., & Kraut, J. (1990a) *Biochim. Biophys. Acta 1038*, 90–97.

Vitello, L. B., Huang, M., & Erman, J. E. (1990b) *Biochemistry 29*, 4283–4288.

Vitello, L. B., Erman, J. E. Miller, M. A., Mauro, J. M., & Kraut, J. (1992) *Biochemistry 31*, 11524–11535.

Vitello, L. B., Erman, J. E., Miller, M. A., Wang, J., & Kraut, J. (1993) *Biochemistry* (following paper in this issue).

Wang, J., Mauro, J. M., Edwards, S. L., Oatley, S. J., Fishel, L. A., Asford, V. A., Xuong, N. H., & Kraut, J. (1990) *Biochemistry 29*, 7160–7173.

Xuong, N.-H., Nielsen, C. P., Hamlin, R., & Anderson, D. H. (1985) *J. Appl. Crystallogr. 18*, 342–350.

Yonetani, T., & Schleyer, H. (1967) *J. Biol. Chem. 242*, 1974–1979.